International Immunopharmacology 71 (2019) 68–75

Contents lists available at ScienceDirect

International Immunopharmacology

journal homepage: www.elsevier.com/locate/intimp

LncRNA analysis of lung tissues after hUC-MSCs and FTY720 treatment of lipopolysaccharide-induced acute lung injury in mouse models

Xia Zhang[a,c,1], Huiying Liu[b,1], Shiyu Wang[a,c], Zihao Huang[a,c], Herong Wang[c,d], Wenkai Niu[b], Yanhong Qin[b], Changqing Bai[b,*], Gang Liu[c,*], Huipeng Chen[c]

[a] Institute of Physical Science and Information Technology, Anhui University, Hefei 230601, China
[b] Department of Respiratory and Critical Care Diseases, 307 Hospital of PLA, Beijing 100071, China
[c] Academy of Military Medical Sciences, Beijing 100850, China
[d] College of Life Sciences, Jilin University, Changchun 130012, China

ARTICLE INFO

Keywords:
Acute lung injury (ALI)
Long non-coding RNA (lncRNAs)
hUC-MSCs
Pathway analysis
Transcription factor

ABSTRACT

Acute lung injury (ALI), a persistent lung inflammatory response syndrome, may evolve into acute respiratory distress syndrome (ARDS). Characterized by rapid onset, critical features, and a complex etiology, ALI remains a challenging critical respiratory disease. Recently, mesenchymal stem cells (MSCs) have provided a new solution for the treatment of ALI. We built a lipopolysaccharide (LPS)-induced ALI model in mice. After treatment with human umbilical cord mesenchymal stem cells (hUC-MSCs), FTY720, or a combination of hUC-MSCs and FTY207, the lung inflammatory response was apparently attenuated. To understand the mechanism underlying MSCs treatment of ALI at the genetic level, significant differentially expressed long non-coding RNAs (lncRNAs) between the treatment and model groups were analyzed using microarray technology. Moreover, genetic gene prediction, gene ontology (GO) analysis, pathway analysis, and transcription factor (TF) prediction were carried out. The results showed that a total of 66 lncRNAs were differentially expressed in all three treatment groups, including 8 up-regulated and 58 down-regulated lncRNAs. LncRNA A_30_P01029806 and A_30_P01029194, which were down-regulated, were involved in the signaling pathways closely related to ALI. Through further TF analysis, we identified several significant TFs which lay a foundation for revealing the mechanism underlying lncRNAs treatment of ALI. LncRNA A_30_P01029806 and A_30_P01029194 may serve as candidate biomarkers in the diagnosis and treatment of ALI.

1. Introduction

Acute lung injury (ALI) is an acute condition of alveolar-capillary membrane damage caused by various intra- and extra-pulmonary pathogenic factors other than cardiogenic factors. End-stage ALI is defined as acute respiratory distress syndrome (ARDS), which is known for its complex etiology, rapid progression, and high mortality. ARDS still poses a challenge for the treatment of critical respiratory diseases. The currently available treatment for ALI/ARDS is respiratory support technology, and no specific medication therapy has been shown to be effective. Therefore, new treatment pathways and solutions are urgently needed for ALI/ARDS.

With progress in medical research, treatments for ALI/ARDS focused on cellular, molecular, and genetic levels. Due to advances in functional assessment of stem cells, mesenchymal stem cells (MSCs) provide an ideal source for tissue repair and have received growing attention for use in the treatment of ALI/ARDS. MSCs have been proven to be effective for attenuating lung injury induced by different factors because of anti-inflammatory, anti-apoptotic, anti-fibrotic, anti-oxidative, and immumomodulatory effects, as well as angiogenetic activity and the power for driving tissue regeneration [1–4]. For these advantages, MSCs are believed to be a promising prospect for the treatment of immune system diseases, although the molecular mechanisms underlying MSCs action are unknown for some diseases.

In recent years, long non-coding RNAs (lncRNAs) have become a focus of research in relation to the pathogenesis of different diseases. LncRNAs are a type of non-coding RNA(ncRNA) that exceeds 200 nucleotides in length and are considered dark matter in the genome [5]. Existing studies have shown that lncRNAs exert extensive regulatory effects in each step of gene expression, including epigenetic,

* Corresponding authors.
E-mail addresses: mcp1604@sina.com (C. Bai), jueliu@sohu.com (G. Liu).
[1] These authors contributed equally to this study.

https://doi.org/10.1016/j.intimp.2019.03.017
Received 3 January 2019; Received in revised form 10 February 2019; Accepted 6 March 2019
Available online 14 March 2019

transcriptional, and post-transcriptional levels. A growing body of evidence indicates that lncRNAs, with features of high diversity, cell-specific distribution, and evolutionary conservation, can serve as biomarkers for disease diagnosis. LncRNAs can also be used as key node molecules in some specific pathways for developing targeted drugs. Wang et al. [6] found through methylation analysis of lncRNA genes that lncRNA EPIC1 interacts with MYC, thus promoting tumor cell growth. According to Wang et al. [7], lncTCF7 plays an important role in maintaining self-renewal of liver cancer stem cells and may be the potential target for tumor intervention.

With respect to the treatment of lung injury, some progress has been made in the functions of lncRNAs. LncRNA MALAT1 knock-out can inhibit LPS-induced acute lung injury by up-regulating miR-146a [8] and can relieve acute lung injury by regulating the NF-κB and p38-MAPK signaling pathways via TLR4 [9]. Lnc-IL7R, an inflammatory regulator, is a novel biomarker for the diagnosis of ARDS and prediction of severity and 28-day mortality [10]. LncRNA CASC2 has been shown to improve ALI by regulating the miR-144-3p/AQP1 axis and reducing the apoptosis of lung epithelial cells [11]. Deep investigation into the biological functions of lncRNAs will elucidate the pathogenesis of ALI/ARDS and identify new diagnostic and treatment biomarkers for ALI/ARDS.

Our preliminary research indicated that hUC-MSCs, FTY720 or a combination of hUC-MSCs and FTY720 attenuate LPS-induced ALI in mice, but the mechanism of action is unclear. To study the treatment and recovery mechanism of ALI, we applied the bioinformatics technique to compare differentially expressed lncRNAs between the treatment and model groups. Target gene prediction, gene ontology (GO) analysis, pathway analysis, and functional annotation of differentially-expressed lncRNAs were performed. Possible lncRNAs related to ALI treatment were identified and TFs involved in ALI were predicted. Our research findings provide the theoretical basis for the development of multiple gene targets or combined medication therapy for ALI/ARDS.

2. Materials & methods

2.1. Ethical statement

The research procedures were approved by the Affiliated Hospital of Military Medical Science Scientific Research Ethics Committee (IRB Approval number: ky-2015-3-7).

2.2. Laboratory animals

Healthy male C57BL/6 mice, 8–10 weeks of age and weighing 18–22 g, were purchased from Beijing HFK Bioscience Co., Ltd. (laboratory animal license: SCXK [Beijing] 2014–0004; Beijing, China). The mice were allowed free access to food and water (Laboratory Animal Center of the Academy of Military Medical Sciences, Beijing, China). All animal experiments conformed to the NIH Directive (NIH Publication No. 85-23, revised 2011; Guide for the Care and Use of Laboratory Animals). The mice were randomly divided into the following five groups (n = 15 for each group): normal control; ALI model [P] (LPS + PBS); hUC-MSCs treatment [M] (LPS + hUC-MSCs); FTY720 treatment [F] (LPS + FTY720); and hUC-MSCs plus FTY720 treatment [FM] (LPS + hUC-MSCs + FTY720). At the end of treatment, all mice were euthanized.

2.3. Establishment of the ALI mouse model and treatment

For each mouse, a 0.5% sodium pentobarbital solution was injected intraperitoneally to induce anesthesia and *Escherichia coli* O55:B5 LPS (10.0 mg/kg [50 μL]; Sigma, St. Louis, MO, USA) was instilled intratracheally. Twenty-four hours later, 200 μL of sterile PBS was injected via the tail vein in the model group. For the hUC-MSCs and hUC-MSCs + FTY720 groups, 2×10^5hUC-MSCs in 200 μL were injected into each mouse via the tail vein. hUC-MSCs was obtained from the 307-IVY Translation Medicine Center (Laboratory of Oncology, Affiliated Hospital of Academy of Military Medical Sciences, Beijing, China). For the FTY720 and hUC-MSCs + FTY720 groups, 0.1 mg/kg of FTY720 was injected intraperitoneally for each mouse in a volume of 200 μL (Sigma).

2.4. Efficacy assessment

Forty-eight hours after LPS instillation, the inflammatory status of the lung was examined using a micro CT scanner (PerkinElmer-Caliper LS, Co., Boston, MA, USA). The left lung was harvested for HE staining and pathohistologic analysis. The dry-to-wet weight ratio was measured for the right lung. Levels of total proteins and inflammatory factors in the bronchoalveolar lavage fluid were determined [12].

2.5. RNA extraction

Part of the left lung tissue was selected for pathological analysis and the therapeutic effect evaluation. At the same time, RNA from the remaining lung tissue were extracted and performed lncRNA analysis. 3 samples were taken from each group, the control group was numbered P1–3, and the experimental group numbers were M1–3, F1–3, MF1–3. Total RNA extraction was performed using Trizol reagent in the remaining lung tissues (Invitrogen, Carlsbad, CA, USA). A NucleoSpin® RNA Clean-up kit (Macherey-Nagel, Düren, Germany) was used for purification of the extracted RNA by passing through the column. RNA quantification was performed using a spectrophotometer. RNA purity and integrity.

2.6. Microarray analysis

Double-stranded complementary DNA (cDNA) was synthesized in accordance with the manufacturer's instructions and fluorescently labeled (Corecore® cDNA amplification labeling kit; CapitalBio Corporation, China). The labeled cDNA was hybridized to Mouse (V2) Gene Expression Microarray8x60K (Agilent, Santa Clara, CA, USA). The microarray was scanned using an Agilent G2565CA Microarray Scanner to obtain the hybridized microarray images, which were then pre-processed with Feature Extraction software to convert the image signals into digital signals. The original data were input into GeneSpring GX software. The signal values were normalized using a percentile shift algorithm and analyzed statistically. P values from the *t*-test and fold-change (FC) were used to identify the differentially-expressed lncRNAs. A Fc ≥ 1.5 and a P ≤ 0.05 were applied to the up- or down-regulated lncRNAs. Data for the expression of lncRNAs were normalized and clustered using CLUSTER 3.0 software.

2.7. Prediction of target genes for lncRNAs

LncRNA-mRNA correlation analysis was performed between expression of lncRNAs differentially expressed in all three treatment groups (M, F, and MF) and microarray mRNA expression. The normalized signal values of each sample in each probe were used as a data source to calculate pairwise correlations and to verify the assumptions. Correlation coefficients and P values were obtained. Pearson's correlation coefficient was calculated with the following the criteria: correlation > 0.99 or < −0.99; and a P-value < 0.05. Based on an analysis of the lncRNA-mRNA co-expression profile, co-expressed lncRNA-mRNA pairs within a distance of 10 kb in the genome were identified based on the cis-regulatory effect. The top 1000 pairs with the highest correlations in the target gene prediction were chosen to draw the network graph with Cytoscape software.

2.8. Functional enrichment analysis of target genes for lncRNAs

GO and pathway enrichment analyses were performed based on the results of target gene prediction. The roles of abnormally-expressed mRNAs in GO entries and signaling pathways were the analyzed. GO entries provide a standardized description of gene products from the perspective of cellular components, molecular function, and biological processes. The number of differentially-expressed genes in each GO entry was calculated. The significance of differentially-expressed genes enriched for each GO entry and signaling pathway was determined by statistical testing. The calculated results were given in the form of P values for the significance of enrichment. A $P \leq 0.05$ indicated that the differentially-expressed genes were significantly enriched for the specific GO entry or signaling pathway.

2.9. Prediction of TFs for lncRNAs

Based on target gene prediction and using the public version of the MATCH™ tool, the TF binding sites were predicted from the 2000 bp upstream to the 500 bp downstream of the lncRNA transcriptional start site (TSS). All predicted results with the highest degree of correlation were chosen. The lncRNAs-transcription factor regulatory network was drawn with Cytoscape.

3. Results

3.1. Construction of the ALI mouse model and hUC-MSCs and FTY720 treatment models

Forty-eight hours after LPS-stimulated induction of ALI, a CT scan of the lung tissues was performed. There was an apparent lung deformity and damage in the model group, with edema, enlargement, and larger and a greater number of bleeding points in the lung tissues. Pathologic analysis indicated alveolar enlargement and thickening of lung tissues in mice with ALI. All three treatment groups showed improved lung morphology compared with the control group. Lung damage was least severe in the hUC-MSCs plus FTY720 treatment group, which exhibited the most attenuated inflammatory response [12].

3.2. RNA quality control

The sectioned lung tissues were stained and measured for the dry-to-wet weight ratio. The remaining lung tissues were subjected to total RNA extraction using Trizol reagent. The OD260-to-280 ratio was 1.9:2.1 and the total amount of extracted RNA in each group was > 10 μg. The bands obtained by denaturing formaldehyde agarose gel electrophoresis were clear and the brightness ratio of the28SrRNA band-to-18S rRNA was close to 2:1. The quality, purity, and integrity of RNA extracted from the lung tissues met the requirements for microarray profiling.

3.3. Identification of differentially-expressed lncRNAs in lung tissues of ALI mice after treatment

The scatter plot shows the differences in gene expression in the lung tissues between the treatment and ALI groups. As compared with the ALI group, there were 559 differentially-expressed lncRNAs in the hUC-MSCs treatment group, with 124 up-regulated and 435 down-regulated. The FTY720 treatment group had 398 differentially-expressed lncRNAs, with 74 up-regulated and 324 down-regulated. The hUC-MSCs plus FTY720 treatment group had 756 differentially-expressed lncRNAs, with 44 up-regulated and 712 down-regulated ($FC \geq 1.5$ and $P \leq 0.05$; Fig. 1A–C). According to a Venn diagram, 66 differentially-expressed lncRNAs were shared among the three treatment groups (Fig. 1D), with 8 up-regulated and 58 down-regulated (Table S1). Clustering of the shared differentially-expressed lncRNAs among the three treatment groups showed that the lncRNAs discriminated between the control and treatment groups. The expression of lncRNAs was significantly different before and after treatment (Fig. 1E). A Circos diagram was created for the shared lncRNAs for the hUC-MSCs plus FTY720 treatment (MF), which clearly displayed the position, down-regulation, or up-regulation and FC of the lncRNAs in the mouse genome (Fig. 2).

3.4. Target gene prediction and functional enrichment analysis of lncRNAs

Because lncRNAs do not encode proteins, the biological functions of lncRNAs should be annotated through other means. To achieve this end, the co-expressed encoding genes should be calculated for the differentially-expressed lncRNAs. By establishing the lncRNA-mRNA regulatory network, the function of lncRNAs can be inferred and annotated from the mRNAs with known functions. GO and pathway enrichment analyses were performed for the target genes for lncRNAs predicted based on co-expression (Fig. S1). Through GO function annotation, it was shown that the target genes were mainly related to the biological processes of single-multicellular organisms, signaling, and regulation of I − κB kinase/NF − κB signaling. The GO category of cellular components was closely associated with dendritic spine membranes for these target genes (Fig. 3A). Pathway analysis revealed the metabolic pathways undergoing significant changes throughout the experiment. As indicated by the results, the differentially-expressed lncRNAs were mainly related to the following signaling pathways: interleukin (IL)-6 family; VEGF; Jak − STAT; and TGF-β. IL-6 is considered a reliable severity indicator of local lung tissue damage, which reflects the treatment efficacy in pulmonary contusion objectively and effectively [13] (Fig. 3B).

Based on the results of lncRNA-mRNA co-expression (Fig. S1), the degree of lncRNA A_30_P01029806 and A_30_P01029194 was higher. Of note, the degree of a lncRNA or a gene is defined as the number of other genes that interact with it, which is shown by the size of its cycle node. This finding indicated that a large number of target genes were predicted (Table 1). All signaling pathways involving these target genes were identified by search and comparison. We found that lncRNAA_30_P01029806 was mainly involved in the IL-6 family, TGF-β, and Jak-STAT signaling pathways. A_30_P01029194 played a role in the VEGF signaling and arginine and proline metabolism pathways (Table 2). These signaling pathways might be associated with ALI.

3.5. Prediction of TFs for lncRNAs

To further discuss the possible upstream regulatory mechanism for the differentially-expressed lncRNAs (A_30_P01029806 and A_30_P01029194), the TFs were analyzed. The potential TF binding sites were predicted near the TSS of the nuclear gene for lncRNAs using the MatchTM algorithm. The relationships between TFs and lncRNAs were derived, and the lncRNA-TF network (Fig. 4) and lncRNA-mRNA-TF network (Fig. S2) were established. As seen from the networks, Myog, Foxj2, NFATC2, and Pitx1 were involved in regulation of lncRNA A_30_P01029806. Tcf12, Sox5, and Ahr:Arnt were involved in regulation of lncRNA A_30_P01029194. Arid3a, Nkx2–5, and Myog regulated both of the differentially-expressed lncRNAs. Furthermore, lncRNAs with a higher degree received regulation from several TFs at the same time and regulated the expression of a group of mRNAs. The interactions of such tertiary regulatory circuits were conducive to the amplification, attenuation, and maintenance of the gene regulatory network signals, thus eliciting the appropriate cellular response to the external stimuli. Investigation into the inflammatory cells, cytokines, and gene regulatory circuit involved in ALI/ARDS is essential in developing novel drugs and molecular targets for treatment.

4. Discussion

ALI and ARDS, characterized by high morbidity and mortality, have

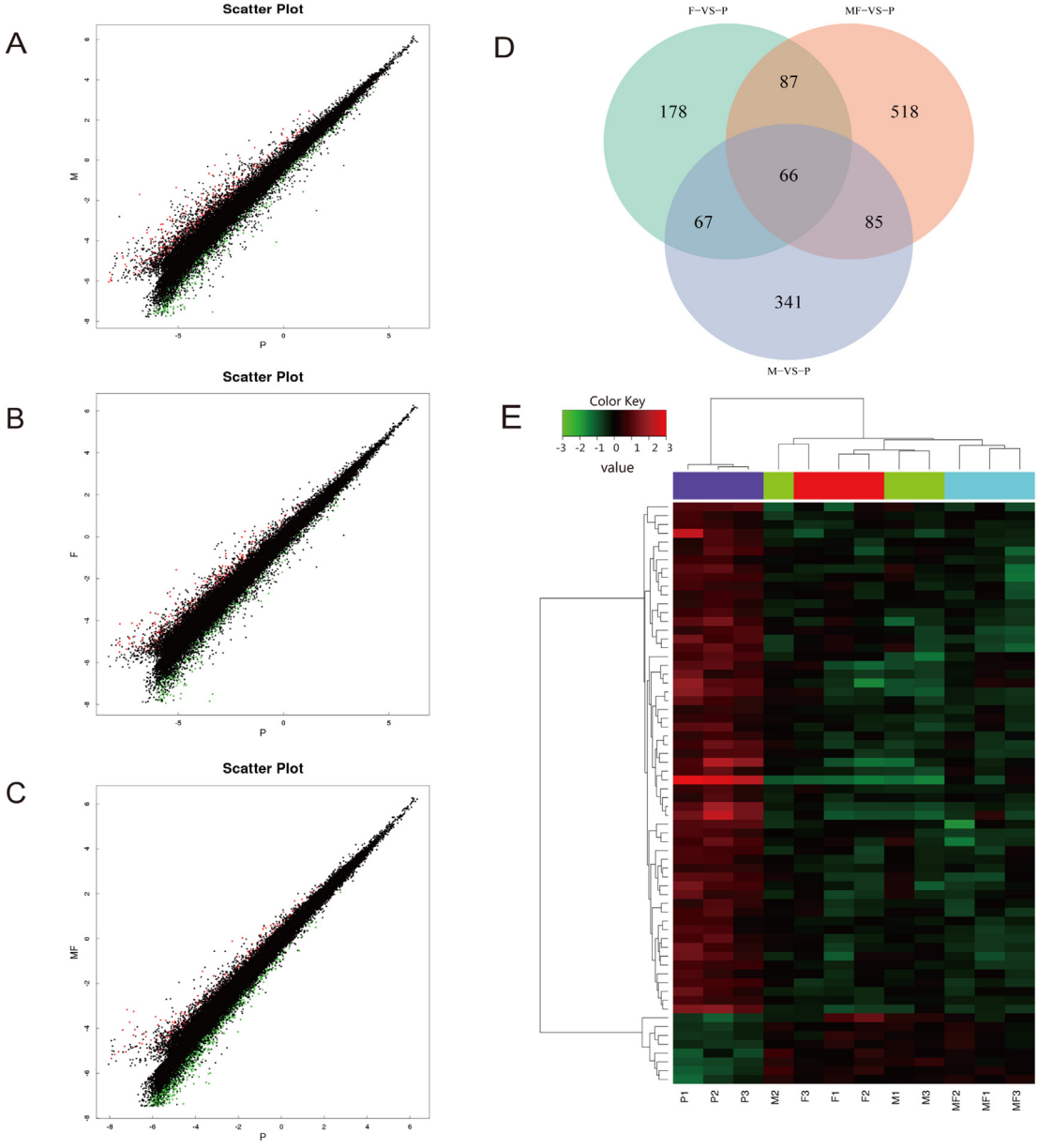

Fig. 1. Screening and clustering of differentially-expressed lncRNAs.
(A), (B), and (C) are scatter plots for the differentially-expressed lncRNAs in P vs. M, P vs. F, and P vs. MF treatments, respectively. The X and Y axes represent the means of standard values for lncRNA in each sample from the ALI and treatment groups, respectively. Red represents the up-regulated genes, green represents the down-regulated genes, and black represents the insignificant differentially-expressed genes. (D) A Venn diagram showing the amount of differentially-expressed lncRNAs in the three treatment groups. There were 66 differentially-expressed lncRNAs occurring in all 3 treatment groups, 8 of which were up-regulated and 58 of which were down-regulated. (E) Clustering diagram of the differentially-expressed lncRNAs shared in the three treatment groups. The color scale represents the different expression of genes from low-to-high, with green representing down-regulated and red representing up-regulated. P: PBS control (LPS + PBS) group; M: hUC-MSCs treatment (LPS + hUC-MSCs) group; F: FTY720 treatment (LPS + FTY720) group; MF: hUC-MSCs plus FTY720 treatment (LPS + hUC-MSCs + FTY720) group. (For interpretation of the references to color in this figure legend, the reader is referred to the web version of this article.)

long been foci of research. As a result of the response and interactions between multiple inflammatory mediators, ALI and ARDS occur when the dynamic balance between the pro- and anti-inflammatory cytokines is disrupted, leading to a severe inflammation cascade reaction. According to existing clinical trials, the severe pathologic injury induced by ALI cannot be reversed by a single drug. Currently, increasing attention has been drawn to the use of cell therapy in ALI and ARDS, especially MSCs. A wide array of cytokines secreted by MSCs as a pluripotent stem cell exert a systemic regulatory effect; however, the mechanism underlying MSC treatment for ALI and ARDS remains largely unclarified.

LncRNAs are a novel heterogenous group of ncRNAs consisting of intronic/exonic lncRNAs, antisense lncRNAs, overlapping lncRNAs, and long intergenic non-coding RNAs (lincRNAs). In ncRNAs, both lncRNAs and miRNAs show strong tissue specificity and are found to be associated with a large number of complex diseases. However, miRNAs are very short and have a single mechanism of action. Usually its specificity is poor, with hundreds of target genes. As a disease diagnosis and treatment, the prospects are not as good as lncRNAs. Compared with miRNAs, the mechanism of gene regulation by lncRNAs is more complex, more extensive and more flexible. LncRNAs, as an important component, can participate in the whole network of gene expression regulation by interacting with miRNAs, transcription factors and epigenetic modification factors. It can achieve extensive and efficient

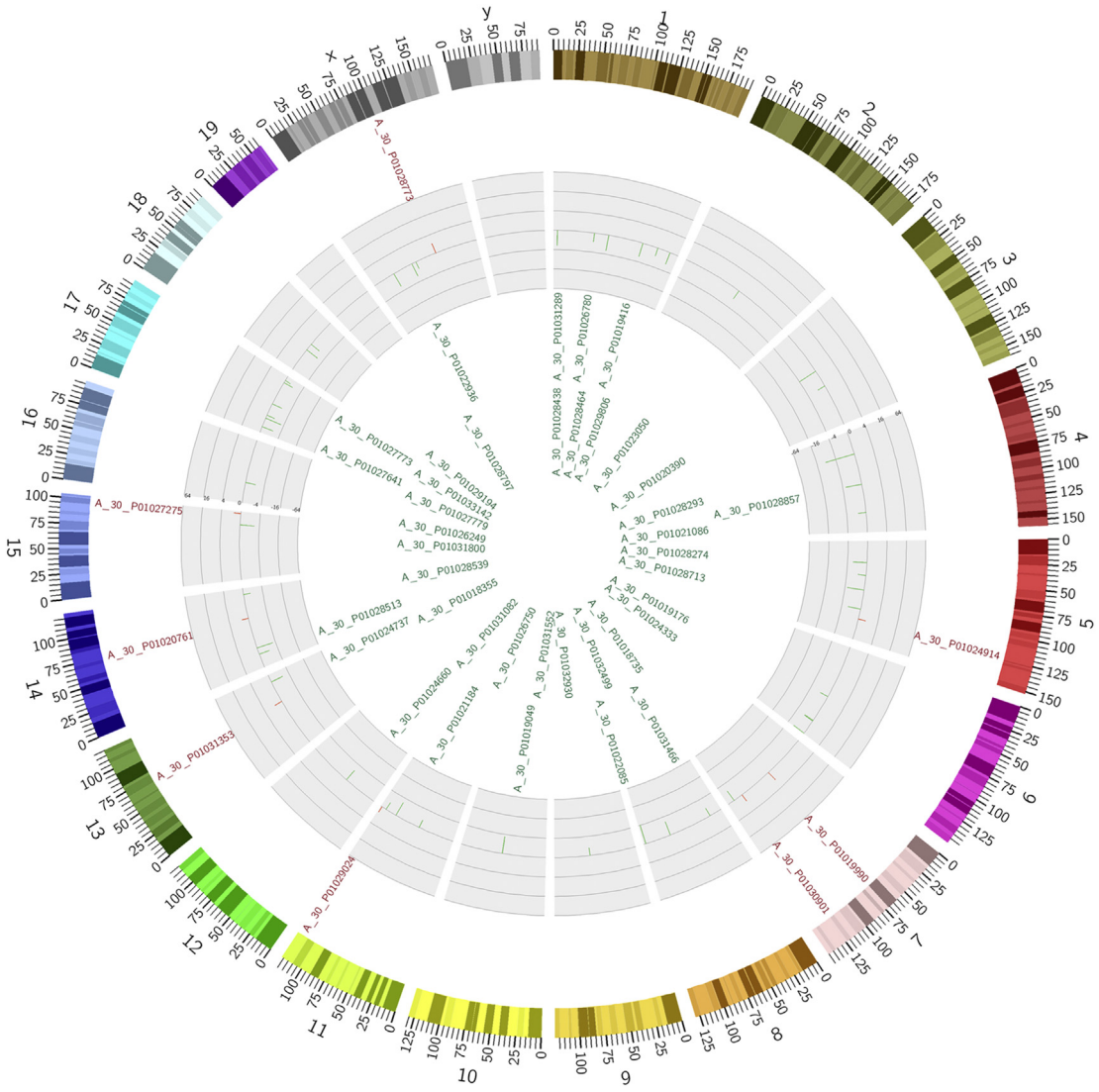

Fig. 2. Distribution of differentially-expressed lncRNAs in the mouse genome.
In the outer-inner direction, the first ring represents the chromosome map of the mouse genome, with color blocks in different shades indicating chromosome cytobands. The second ring represents the FC and P values of the shared differentially-expressed lncRNAs in the MF treatment group, with green representing down-regulated and red representing up-regulated. (For interpretation of the references to color in this figure legend, the reader is referred to the web version of this article.)

regulation of gene expression from the pre-transcriptional crystal, transcriptional level and post-transcriptional level. They are closely related to cell cycle and differentiation, development, reproduction, sex control, ageing, and many human diseases. In recent years, lncRNA studies in relation to lung damage have facilitated a new understanding about the pathogenesis of ALI and ARDS, opening up a new prospect for the diagnosis and treatment of ALI and ARDS.

For the first time, stem cell therapy, ALI and ARDS, and lncRNAs were linked together in the current study, and the differential expression of lncRNAs before and after the treatment for ALI and ARDS were analyzed. The treatment efficacy was assessed. As compared with the model group, the severity of lung damage was significantly lessened in the treatment groups, with the greatest attenuation found in the hUC-MSCs plus FTY720 treatment. A bioinformatics technique was applied to the differentially-expressed lncRNAs in the treatment and model groupsat the transcriptional level. As is seen in Fig. 1D, the Venn diagram shows the hUC-MSCs plus FTY720 treatment resulted in the highest number of differentially-expressed lncRNAs(n = 756) in the mouse lung tissues, with down-regulated genes accounting for 94.18%. Combined with pathological outcomes, we can conclude that hUC-MSCs down-regulates cellular pro-inflammatory factors to relieve symptoms of lung injury and the combination of the hUC-MSCs + FTY720 can amplify this influence to get better treatment results. Microarray analysis indicated that the higher the number of differentially-expressed genes, the more significant the relief of the lung damage. The predominance of the down-regulated genes implies that combined therapy was most effective in inhibiting the inflammation cascade in ALI mice.

To clarify the role of lncRNAs in the treatment of ALI and ARDS, we applied microarray analysis to the differentially-expressed lncRNAs in the three treatment and model groups. The results showed that 66 lncRNAs were differentially-expressed in all three treatment groups. According to cluster analysis, the differentially-expressed lncRNAs were involved in the regulation of ALI, and thus may serve as potential targets for the treatment of ALI. This result agrees with the fact that ALI and ARDS is a systemic disease that cannot be treated via a single target. Next, the target genes were predicted based on co-expression, and functional annotation and TF prediction were carried out to understand the functional distribution and mechanism underlying the lncRNAs.

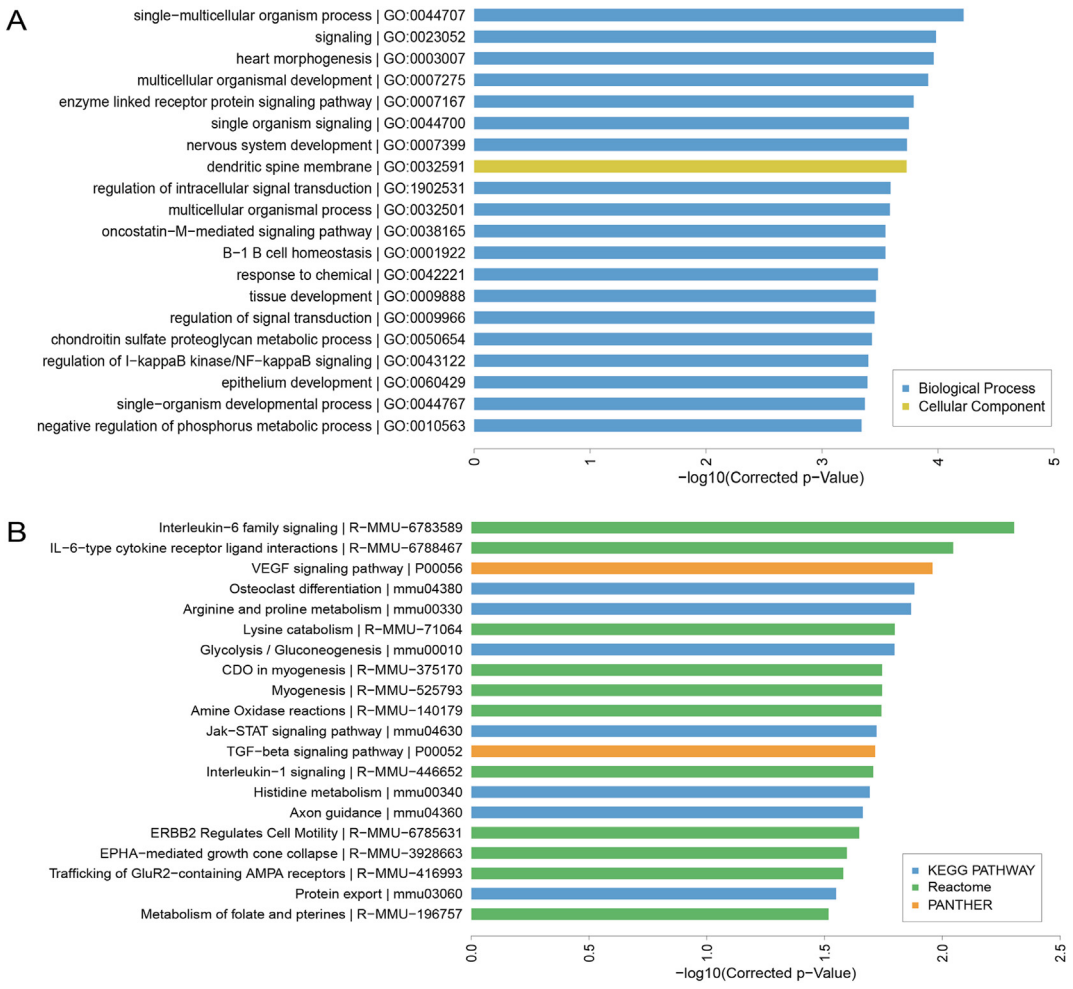

Fig. 3. GO and pathway analysis of differentially-expressed lncRNAs.
(A) shows the GO categories of biological processes for the lncRNA target genes. P values were obtained by the Fisher's exact test and the significant functions were annotated for the target genes for lncRNAs. (B) shows the KEGG pathways and PANTHER classifications of the target genes for lncRNAs. Correlation analysis was performed for the discrete distribution of genes in the pathways to obtain the pathway categories significantly correlated to ALI.

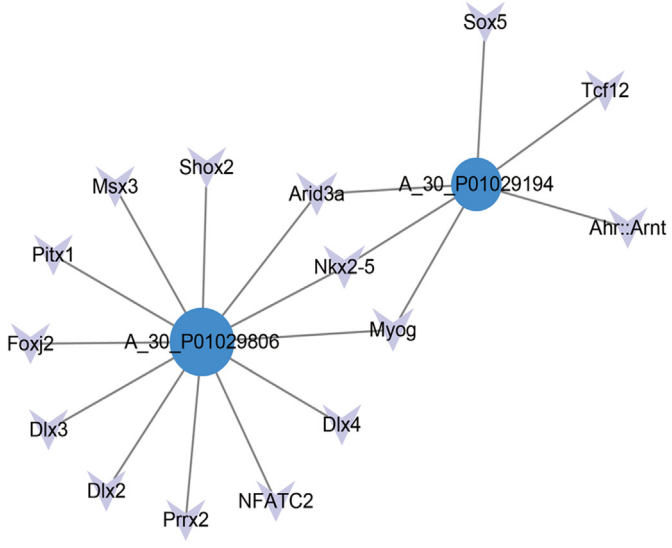

Fig. 4. lncRNA-TF network.
Blue represents lncRNA and purple represents TF, with the dot size indicating the degree of lncRNA. (For interpretation of the references to color in this figure legend, the reader is referred to the web version of this article.)

LncRNA A_30_P01029806 was down-regulated in each treatment group and shown to be related to IL-6 family, TGF-β, and Jak-STAT signaling pathways. IL-6 is a pleiotropic cytokine with multiple biological activities and plays an important role in immune and inflammatory responses. IL-6 content is higher in the lung and blood of ARDS patients than healthy subjects, and can be utilized to reflect the severity of local lung damage. Several studies have shown that transforming growth factor (TGF)-β1, as a novel target for the prevention and treatment of radiation-induced lung damage, exists at higher levels in the peripheral blood of patients with radiation-induced lung damage than healthy subjects. Intervention of the TGF-βsignaling pathway can alleviate radiation-induced lung damage [14,15]. The Janus activated kinase(Jak) signal transducers and activators of transcription (STAT) signaling pathway can be activated by cytokines, hormones, and growth factors, which further induce cell proliferation, differentiation, apoptosis, and immune dysregulation. After LPS treatment, activation of STAT occurs earlier than the symptoms of acute lung damage, thus blocking or attenuating the Jak-STAT pathway to shut down the downstream cytokine signals [16,17]. In ALI and ARDS, the JAK/STAT signaling pathway is associated with the MAPK, NF-κB, and PI-3 signaling pathways in various ways, and the cascade response between the pathways is very complex [18]. We suggest that the expression of lncRNA A_30_P01029806 can be used to diagnose the severity and treatment effect of ALI and ARDS. Thus, down-regulation of lncRNA A_30_P01029806 is associated with an attenuation of ALI and ARDS.

Table 1
Two differentially-expressed lncRNAs identified.

Probe name	Primary accession	Number of target genes	FC (abs)			Regulation
			(M vs P)(F vs P)(MF vs P)			
A_30_P01029806	chr1:162965309-162970704_R	371	2.538137	2.81797	1.776127	Down
A_30_P01029194	chr18:46962676-46962824_F	126	3.675554	4.28189	2.116257	Down

Table 2
ALI-related signaling pathways and target genes involving the differentially-expressed lncRNAs.

Probe name	Pathway term	input_gene
A_30_P01029806	Interleukin-6 family signaling	Osmr, Socs3, Osm, Lif
	TGF-beta signaling pathway	Smad9, Nodal, Bmp3, Atf2
	Jak-STAT signaling pathway	Osmr, Socs3, Osm, Lif
		Ptpn2, Pim1, Fhl1, Epor
A_30_P01029194	VEGF signaling pathway	Hspb2, Lpxn
	Arginine and proline metabolism	Maoa, mox

Blocking or reducing the expression of lncRNA A_30_P01029806 is conducive to the treatment of ALI and ARDS.

In addition, lncRNA A_30_P01029194 was down-regulated in each treatment group and associated with several signaling pathways (VEGF signaling & arginine and proline metabolism pathways). The VEGF signaling pathway is related to the proliferation and migration of vascular endothelial cells, changing vascular permeability, controlling angiogenesis, and possibly inducing the inflammatory response [16,17,19]. It has been shown that MSCs lower pulmonary vascular permeability by maintaining sufficient VEGF in the lung, which is conducive to the treatment of rat ALI [20]. In addition to the VEGF signaling pathway, the amino acid metabolism pathways involving lncRNA A_30_P01029194 are also potential treatment targets for ALI. In another study that used the LPS-induced ALI rat model, L-arginine protected against the induced ALI by up-regulating pulmonary surfactant and inhibiting the inflammatory transmitters in alveolar macrophages [21]. We therefore are of the opinion that down-regulation of lncRNA A_30_P01029194 is associated with the up-regulation of VEGF and L-arginine, which leads to enhanced pulmonary vascular integrity and protection against lung damage. LncRNA A_30_P01029194 is another potential treatment target for ALI.

Based on the diversity and regularity of the lncRNA expression pattern identified from microarray analysis, we attempted to uncover the upstream regulatory mechanism of the differentially-expressed lncRNAs from the perspective of TF. For the two lncRNAs of interest, TFs were predicted and the lncRNA-TF network was established. It was easy to find that some TFs may play an important role in the regulation of target genes offered by lncRNAs, which further attenuate ALI. Among the TFs, nuclear factor of activated T-cells 2 (NFATC2), the TF for lncRNA A_30_P01029806, is a calcium-dependent nuclear TF, the activation of which stimulates the proliferation of vascular smooth muscle cells [22,23]. DNA methylation of short stature homeobox 2 (Shox2) has become a biomarker for the early diagnosis of lung cancer [24]. Aryl hydrocarbon receptor: AhR nuclear transporter (Ahr: Arnt), the TF for lncRNA A_30_P01029194, can form a dimer which recognizes and binds to the Ahr/Arnt element and is involved in immunity and bacterial lipopolysaccharide (LPS)-mediated responses in vivo [25]. Moreover, the AhR signaling pathway intersects with the MAPK signaling pathway [26], which further affects the occurrence of inflammatory responses. ALI is induced by a multiplicity of factors and has a complex pathogenesis. The above identified TFs may serve as treatment targets for ALI, but further investigation is needed to understand the specific regulatory mechanism underlying lncRNAs and TFs on ALI.

In summary, pathway analysis indicated that a complex regulatory network comprised of multiple signaling pathways contribute to the development of ALI. These two lncRNAs (lncRNA A_30_P01029806 and lncRNA A_30_P01029194) were involved in the regulation of multiple signaling pathways, not a single target (see Table 2). These signal pathways had different effects on the occurrence and development of ALI/ARDS in different aspects. Our experimental results showed that a single means can't effectively treat the disease, and we need to treat the disease with multiple targets for multiple treatments. It provided important clues for revealing the intricate interactions between the signaling pathways. After that, TFs were predicted for the two lncRNAs, which laid the basis for revealing the underlying mechanism. Gene therapy and stem cell transplantation represent the future for ALI and ARDS treatment; however, further investigation is needed to determine the regulatory mechanism and functions of the relevant lncRNAs in ALI in the hope of identifying new, effective biomarkers and targets for gene therapy for ALI.

The raw data of microarray profiles were uploaded to Figshare, researchers can view them at https://doi.org/10.6084/m9.figshare.7334546.v1.

Supplementary data to this article can be found online at https://doi.org/10.1016/j.intimp.2019.03.017.

Competing interests

All authors declare no competing interests.

Acknowledgements

This project was supported by National Natural Science Foundation of China Project (grant number 31741065), Project for Innovation of Military Medicine (grant number 16CXZ045) and Beijing Nova Program (grant number xx2018052).

We thank Yanbin Zhao and Fangdou Zhang for their help in data analysis and article writing.

References

[1] G. Naveen, K. Anna, K. Maria, M. Majd, T. Xinping, S. Vladimir, M.A. Matthay, Mesenchymal stem cells enhance survival and bacterial clearance in murine Escherichia coli pneumonia, Thorax 67 (6) (2012) 533, https://doi.org/10.1136/thoraxjnl-2011-201176.

[2] Z. Shijia, S.D. Danchuk, I. Kathleen Mp, J.A. Semon, B.A. Scruggs, R.W. Bonvillain, A.L. Strong, J.M. Gimble, A.M. Betancourt, D.E. Sullivan, Comparison of the therapeutic effects of human and mouse adipose-derived stem cells in a murine model of lipopolysaccharide-induced acute lung injury, Stem Cell Res Ther 4 (1) (2013) 13, https://doi.org/10.1186/scrt161.

[3] X. Jiang, J. Xin, Q. Chao, P. Chang, Z. Chu, Y. Qu, Y. Liu, Intravenous delivery of adipose-derived mesenchymal stromal cells attenuates acute radiation-induced lung injury in rats, Cytotherapy 17 (5) (2015) 560–570, https://doi.org/10.1016/j.jcyt.2015.02.011.

[4] I.K., F.S., E.B., T.R., P.-B., D, N.C., R.A., A.S., H.H., H.D., Adipose-derived stem cells attenuate pulmonary microvascular hyperpermeability after smoke inhalation, PLoS One 12 (10) (2017) e0185937. doi:https://doi.org/10.1371/journal.pone.0185937.

[5] E.P. Consortium, Identification and analysis of functional elements in 1% of the human genome by the ENCODE pilot project, Nature 447 (7146) (2007) 799–816, https://doi.org/10.1038/nature05874.

[6] S.J. Caesar-Johnson, J.A. Demchok, I. Felau, M. Kasapi, M.L. Ferguson, C.M. Hutter, H.J. Sofia, R. Tarnuzzer, Z. Wang, L. Yang, lncRNA epigenetic landscape analysis identifies EPIC1 as an oncogenic lncRNA that interacts with MYC and promotes cell-cycle progression in cancer, Cancer Cell 33 (4) (2018), https://doi.org/10.1016/j.

ccell.2018.03.006.
[7] Y. Wang, H. Lei, D. Ying, P. Zhu, G. Huang, J. Luo, X. Yan, B. Ye, L. Chong, P. Xia, The long noncoding RNA lncTCF7 promotes self-renewal of human liver Cancer stem cells through activation of Wnt signaling, Cell Stem Cell 16 (4) (2015) 413–425, https://doi.org/10.1016/j.stem.2015.03.003.
[8] L. Dai, G. Zhang, C. Zhe, W. Xi, L. Jia, X. Jing, H. Wang, Z. Rui, L. Meng, T. Jiang, Knockdown of LncRNA MALAT1 contributes to the suppression of inflammatory responses by up-regulating miR-146a in LPS-induced acute lung injury, Connect. Tissue Res. 2 (2018) 1–12, https://doi.org/10.1080/03008207.2018.1439480.
[9] H. Li, H. Shi, N. Ma, P. Zi, Q. Liu, R. Sun, BML-111 alleviates acute lung injury through regulating the expression of lncRNA MALAT1, Arch. Biochem. Biophys. (2018), https://doi.org/10.1016/j.abb.2018.04.016.
[10] B. Wan, W.J. Xu, W.N. Xu, P. Zhan, G.N. Wu, J.J. Jin, G.M. Xi, J.T. Yin, H. Zhang, Y.K. Chen, Plasma long noncoding RNA IL-7R as a prognostic biomarker for clinical outcomes in patients with acute respiratory distress syndrome, Clin. Respir. J. (2017), https://doi.org/10.1111/crj.12717.
[11] H. Li, H. Shi, M. Gao, N. Ma, R. Sun, Long non-coding RNA CASC2 improved acute lung injury by regulating miR-144-3p/AQP1 axis to reduce lung epithelial cell apoptosis, Cell Biosci. 8 (1) (2018) 15, , https://doi.org/10.1186/s13578-018-0205-7.
[12] Z. Zhang, W. Li, Z. Heng, Z. Jing, P. Li, Y. Xin, W. Niu, C. Bai, H. Liu, Combination therapy of human umbilical cord mesenchymal stem cells and FTY720 attenuates acute lung injury induced by lipopolysaccharide in a murine model, Oncotarget 8 (44) (2017) 77407–77414, https://doi.org/10.18632/oncotarget.20491.
[13] N. Nazim, P. Gavin D, T. William, M. Nick, M. Mav, T. David R, Kerbs von Lungren 6 antigen is a marker of alveolar inflammation but not of infection in patients with acute respiratory distress syndrome, Crit. Care 12 (1) (2008) R12, https://doi.org/10.1186/cc6785.
[14] M.F. Chen, P.C. Keng, P.Y. Lin, C.T. Yang, S.K. Liao, W.C. Chen, Caffeic acid phenethyl ester decreases acute pneumonitis after irradiation in vitro and in vivo, BMC Cancer 5 (1) (2005) 158, , https://doi.org/10.1186/1471-2407-5-158.
[15] A. Mitchell S, T. Bradley, R. Zahid, T. Beverly, V. Zeljko, Antitransforming growth factor-beta antibody 1D11 ameliorates normal tissue damage caused by high-dose radiation, Int. J. Radiat. Oncol. Biol. Phys. 65 (3) (2006) 876–881, https://doi.org/10.1016/j.ijrobp.2006.02.051.
[16] S. Mariano, T. Satoe, L.M. Rozo, R.J. Homer, K. Charles, J.W. Jhung, P. George, S. Michael, P.M. Hassoun, B.L. Fanburg, Activation of the STAT pathway in acute lung injury, Am. J. Physiol. Lung Cell. Mol. Physiol. 286 (6) (2004) 1282–1292, https://doi.org/10.1152/ajplung.00349.2003.
[17] S. Mariano, T. Satoe, T. Powen, P. George, R.J. Homer, J.W. Jhung, B. Deepa, B.H. Cochran, A.R. Simon, Inhibition of the Src and Jak kinases protects against lipopolysaccharide-induced acute lung injury, Am. J. Respir. Crit. Care Med. 171 (8) (2005) 858, https://doi.org/10.1164/rccm.200407-981OC.
[18] Jason S. R., Kristin M. R., Douglas A. H., The JAK/STAT signaling pathway, J. Cell Sci. 117 (8) (2004) 1281–1283, https://doi.org/10.1242/jcs.00963.
[19] K. Kumano, A. Nakao, H. Nakajima, S. Miike, K. Kurasawa, Y. Saito, I. Iwamoto, Blockade of JAK2 by tyrphostin AG-490 inhibits antigen-induced eosinophil recruitment into the mouse airways, Biochem. Biophys. Res. Commun. 270 (1) (2000) 209–214, https://doi.org/10.1006/bbrc.2000.2403.
[20] Y. Yi, S. Hu, X. Xu, J. Li, A. Liu, J. Han, S. Liu, L. Ling, H. Qiu, The vascular endothelial growth factors-expressing character of mesenchymal stem cells plays a positive role in treatment of acute lung injury in vivo, Mediat. Inflamm. 2016 (12) (2016) 1–12, https://doi.org/10.1155/2016/2347938 (2016-5-24) 2016.
[21] L.I. Li-Ping, J.X. Zhang, L.I. Lan-Fang, L.J. Xie, Q.Z. Zhang, N. Hao, L.I. Guo-Feng, Effect of L-arginine on pulmonary surfactant and alveolar macrophages in rats with pulmonary injury induced by lipopolysaccharide, Chinese J. Appl. Physiol. 28 (3) (2012) 263, https://doi.org/10.13459/j.cnki.cjap.2012.03.020.
[22] Z. Wei, K.E. Halligan, Z. Xuexin, J.M. Bisaillon, J.C. Gonzalez-Cobos, R.K. Motiani, H. Guoqing, P.A. Vincent, Z. Jiliang, B. Margarida, Orai1-mediated I (CRAC) is essential for neointima formation after vascular injury, Circ. Res. 109 (5) (2011) 534–542, https://doi.org/10.1161/CIRCRESAHA.111.246777.
[23] D.C. Hill-Eubanks, M.F. Gomez, A.S. Stevenson, M.T. Nelson, NFAT regulation in smooth muscle, Trends Cardiovasc. Med. 13 (2) (2003) 56–62, https://doi.org/10.1016/s1050-1738(02)00212-8.
[24] C. Zhang, W. Yu, L. Wang, M. Zhao, Q. Guo, S. Lv, X. Hu, J. Lou, DNA methylation analysis of the SHOX2 and RASSF1A panel in bronchoalveolar lavage fluid for lung cancer diagnosis, J. Cancer 8 (17) (2017) 3585–3591, https://doi.org/10.7150/jca.21368.
[25] K. Akihiro, N. Tetsuji, N. Taisuke, C. Ichino, M. Kazuya, N. Keiko, F.K. Yoshiaki, K. Tadamitsu, Aryl hydrocarbon receptor in combination with Stat1 regulates LPS-induced inflammatory responses, J. Exp. Med. 206 (9) (2009) 2027–2035 https://www.jem.org/cgi/doi/10.1084/jem.20090560.
[26] S. Chen, T. Operaña, J. Bonzo, N. Nguyen, R.H. Tukey, ERK kinase inhibition stabilizes the aryl hydrocarbon receptor implications for transcriptional activation and protein degradation, J. Biol. Chem. 280 (6) (2005) 4350–4359, https://doi.org/10.1074/jbc.M411554200.